A Physics-Informed Computational Framework for Forward Prediction and Inverse Closure Learning of Pore-Scale Biofilm Growth

Qiang Ye[1, 2], Guangfeng Zhu[1], Qiang Zheng[2], Yu Wu[3], and Lingzao Zeng[1, *]

[1]State Key Laboratory of Soil Pollution Control and Safety, College of Environmental and Resource Sciences, Zhejiang University, Hangzhou 310058, China

[2]Zhejiang Key Laboratory of Industrial Intelligence and Digital Twin, Eastern Institute of Technology, Ningbo, 315200, China

[3]Key Laboratory of Soft Machines and Smart Devices of Zhejiang Province, Department of Engineering Mechanics, Zhejiang University, Hangzhou, 310027, China

* Correspondence to: lingzao@zju.edu.cn

Contents of this file

1. Supplementary Information 1 for Section 2.1 **'Experimental setup and data processing'** in the manuscript.

The specific contents of Supplementary Information

Supplementary Information 1:

The supplementary works in this part include:

(1) Microfluidic chip fabrication, biofilm cultivation and experimental processes

Microfluidic chips were fabricated using soft lithography: the microstructure was designed using AutoCAD® 2023 and fabricated into an optical mask. Using this mask, the chip mold was prepared on a silicon wafer coated with SU8-2050 photoresist in a dust-free laboratory at 20 °C and 60% humidity. In this process, the photoresist on the silicon wafer was exposed to ultraviolet light for 20 seconds using a photolithography machine, developed, and treated with Chlorotrimethylsilane (TMCS) to form the microstructural pattern. Subsequently, PDMS with good optical transparency and chemical inertness was used to cast the mold, which was then cured, cut, and perforated to form the PDMS chip. The glass slide and PDMS chip were cleaned using a plasma cleaner and finally bonded together to form the finished experimental chip. For a detailed process, see Aleklett et al. (2018).

Bacillus subtilis NCIB 3610 was cultured using Luria-Bertani (LB) medium, sterilized by autoclaving at 121 ℃ and 15 psi, with glucose added as the sole carbon source. Bacterial suspensions were prepared and incubated overnight at 37 ℃ with shaking at 220 rpm in light-proof conditions. Prior to injecting bacterial suspensions, the microfluidic system was sterilized sequentially with ultrapure water (18.2 MΩ·cm), 75% ethanol, and phosphate-buffered saline (PBS, pH=7.4). After injection, the *Bacillus subtilis* suspension filled the sealed microfluidic chip and was left for 2 hours to allow the microorganisms to reach irreversible adhesion.

During the experiment, a ChipP01-B syringe pump was used to inject a nutrient solution containing 10 g/L glucose into the microfluidic chip at a Darcy flow rate of 3.93×10^{-5} m/s. The microfluidic chip contains a pore network with dimensions of 8.00 mm (length) × 3.97

mm (width) × 50 μm (height), featuring staggered cylindrical obstacles to mimic a simplified porous structure with a pore-throat diameter of 1.08 mm. Nutrient transport within pore channels governed biofilm growth through coupled physical and biochemical reaction processes. The outlet of the microfluidic chip was open to the atmosphere. During the infusion, a pressure sensor was installed at the inlet of the chip to monitor the pressure, and real-time imaging was performed over 24 hours using an automated inverted microscope (Axio Observer Z1, Zeiss) equipped with a high dynamic range (HDR) camera, capturing 2× 12 tiled fields of view at 3-minute intervals.

(2) Image conversion processing and parameter determination

Based on the Lambert−Beer law (Kurz et al. 2023; Xiong et al. 2020), the grayscale images obtained experimentally are linked to the biomass field through the following formula:

$$M = -\delta ln(I), \tag{S1}$$

where $I\,[-]$ and $M\,[\mathrm{kg/m^3}]$ represent the normalized transmitted light intensity and biofilm density of each pixel space, respectively. $\delta^{-1} = -\epsilon h$, where $\epsilon\,[\mathrm{m^2/kg}]$ is the absorption coefficient of biofilm, and $h\,[\mathrm{m}]$ denotes the optical path length. According to the experimental setup, h is set to 50 μm.

Assuming that M is inversely proportional to the local porosity n, it takes the following form (Kurz et al. 2023):

$$n = (-\beta ln(I))^{-\tau}, \tag{S2}$$

where β is a parameter related to δ and M, and τ is a calibration parameter.

The local porosity n can be converted into the local permeability $k\,[\mathrm{m^2}]$ based on the modified Carman−Kozeny relationship (Chapuis and Aubertin 2003). The equation is expressed as:

$$k = k_h \cdot n^{\omega}, \tag{S3}$$

with k_h being the permeability of the unobstructed microfluidic channel (i.e., the free channel). According to the Hele-Shaw correction (Lamb 1906), k_h is expressed as $k_h = h^2/12 = 2.075 \times 10^{-10}\ \mathrm{m^2}$, which represents the permeability when $n = 1$.

Based on Eqs. (S2)−(S3), the relationship between light intensity I and local

permeability k is derived as follows:

$$k = k_h \cdot (-\beta ln(I) + \gamma)^{-\alpha}, \quad \text{(S4)}$$

where $\alpha = \omega\tau$ and the parameter $\gamma = 1$ ensures that when $I = 1$, $k = k_h$, corresponding to the microfluidic space without biofilm growth (i.e., $n = 1$).

Before determining the characteristic parameter set $(\delta, \beta, \alpha, \tau)$, we need to adhere to the following basic empirical constraints: The porosity of *Bacillus subtilis* biofilm cultivated in the laboratory typically ranges from 0.2 to 0.6 (Lewandowski 2000; Zhang and Bishop 1994). Values below 0.2 represent the detection threshold of the optical instrument, while values above 0.6 indicate the transition to the fluidic region. In this study, the porosity values derived from Eq. (S2) were constrained within this empirical range. Additionally, the maximum biomass of *Bacillus subtilis* observed under laboratory-controlled conditions (Zhang and Bishop 1994) was approximately 10 kg/m^3. Therefore, this value is used as the theoretical maximum biofilm density in our microfluidic experiment (the compression of biofilm is taken into account). Based on these empirical constraints, the characteristic parameters of the biofilm $(\delta, \beta, \alpha, \tau)$ are determined by integrating experimentally monitored data. The normalized light intensity values of biofilm images captured in the experiment fall within the range $I \in [50/255, 220/255]$. Based on Eq. (S2), we can obtain the relationship $n_{max} = 11^{\tau} n_{min}$. To ensure the porosity remains within the empirical range, and assuming that $n_{max} = 3n_{min}$, the value of τ is determined to be 0.45, and β is calculated to be 21.95. For biomass conversion, a scaling parameter of $\delta = 5.0$ was fixed to meet the empirical requirement that biomass does not realistically exceed 10 kg/m^3. This setting ensures smooth conversion between physical quantities while preserving the relative spatial density distribution of biomass. If further calibration of δ is needed, high-precision density measurement techniques can be employed. Additionally, within the selected 69-minute period (Fig. 3a), pressure measurements P_{exp} with no significant experimental errors in the first 45 minutes, are required to inversely determine the characteristic parameter α. The inverse estimation initializes α and computes the permeability field $k(\alpha)$ at each time step using Eq. (S4). The obtained k is then incorporated into COMSOL Multiphysics to simulate the inlet pressure P_{sim}. By coupling MATLAB with COMSOL, the parameter α is iteratively optimized by using the sequential quadratic programming (SQP) algorithm to minimize the

pressure difference $|P_{exp} - P_{sim}|$. The correlation between P_{exp} and P_{sim} is shown in Fig. S1a. Compared to experimental benchmarks, the mean absolute percentage error (MAPE) and the coefficient of determination (R^2) of the simulation are 2.62% and 0.876, respectively. Therefore, the inversely determined α is 2.748. Once all the characteristic parameters $(\delta, \beta, \alpha, \tau)$ are determined, the empirical bounded transformation functions described in Eqs. (S1)–(S4) are used to derive the observation-scale fields (n, M, k). These fields are subsequently used to obtain the initial hydrodynamic and transport fields under steady-state conditions, calibrate the COMSOL model, and provide supervision data for PINN training. The simulated initial velocity (u_0, v_0) and initial substrate concentration C_0 are shown in Fig. S2. Moreover, since biomass, porosity, and permeability fields are observation-scale quantities derived from transmitted light intensity, existing empirical constraints may affect the absolute magnitude of these inferred fields. Therefore, the PINN-based inverse closure learning (see Section 3.4) should be interpreted at the observation scale, rather than as the discovery of a universal microscopic constitutive law.

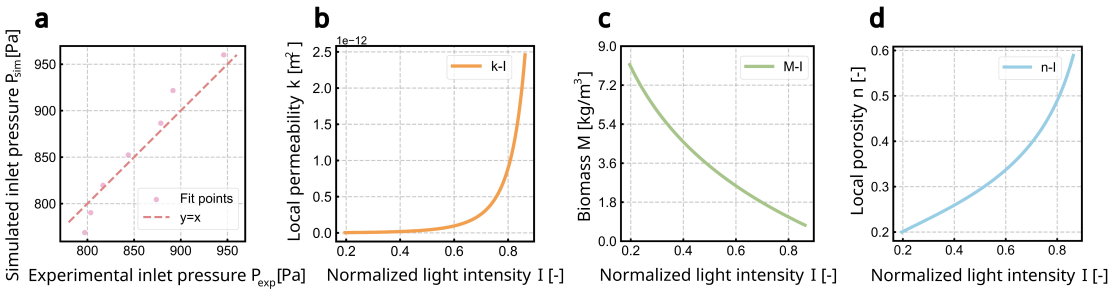

Fig. S1 Data fitting and image-to-property conversion: **a** Correlation between experimental and simulated inlet pressures (P_{exp} and P_{sim}); **b** Relationship between local permeability k and normalized transmitted light intensity I; **c** Relationship between biomass M and I; **d** Relationship between local porosity n and I

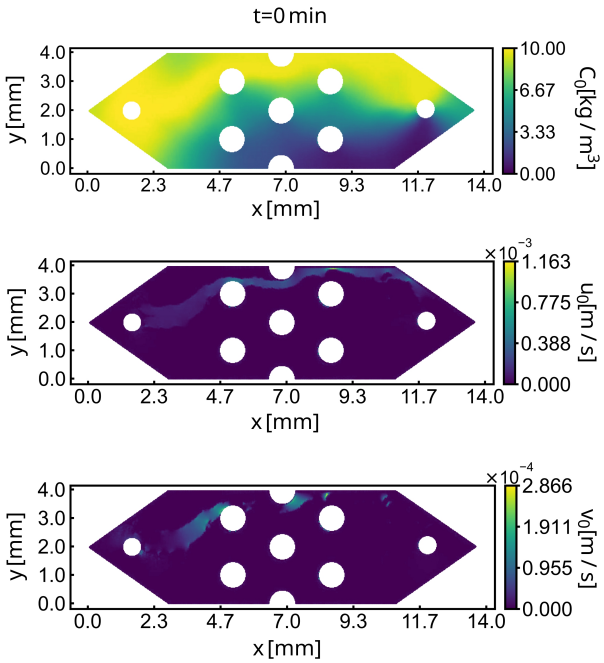

Fig. S2 Simulated initial fields

References

Aleklett, K., Kiers, E.T., Ohlsson, P., Shimizu, T.S., Caldas, V.E., Hammer, E.C.: Build your own soil: exploring microfluidics to create microbial habitat structures. The ISME journal **12**(2), 312–319 (2018). https://doi.org/10.1038/ismej.2017.184

Chapuis, R.P., Aubertin, M.: On the use of the Kozeny Carman equation to predict the hydraulic conductivity of soils. Can. Geotech. J. **40**(3), 616–628 (2003). https://doi.org/10.1139/t03-013

Kurz, D.L., Secchi, E., Stocker, R., Jimenez-Martinez, J.: Morphogenesis of biofilms in porous media and control on hydrodynamics. Environ. Sci. Technol. **57**(14), 5666–5677 (2023). https://doi.org/10.1021/acs.est.2c08890

Lamb, H.: Hydrodynamics (3rd edn). Cambridge University (1906)

Lewandowski, Z.: Notes on biofilm porosity. Water Res. **34**(9), 2620–2624 (2000). https://doi.org/10.1016/S0043-1354(00)00186-X

Xiong, J., Zhuang, P., Zhang, Y.: An efficient underwater image enhancement model with extensive beer-lambert law. In: 2020 IEEE International Conference on Image Processing (ICIP), pp. 893–897. IEEE (2020). https://doi.org/10.1109/ICIP40778.2020.9191131

Zhang, T.C., Bishop, P.L.: Density, porosity, and pore structure of biofilms. Water Res. **28**(11), 2267–2277 (1994). https://doi.org/10.1016/0043-1354(94)90042-6